Effect of Zr on the properties of (TiZr)Ni alloys from first-principles calculations

Q. M. Hu,[1,2,*] R. Yang,[1] J. M. Lu,[1] L. Wang,[3] B. Johansson,[2,4,5] and L. Vitos[2,4,6]

[1]*Shenyang National Laboratory for Materials Science, Institute of Metal Research, Chinese Academy of Sciences, 72 Wenhua Road, Shenyang 110016, China*

[2]*Applied Materials Physics, Department of Materials Science and Engineering, Royal Institute of Technology, Stockholm SE-100 44, Sweden*

[3]*Department of Materials for Special Environment, Institute of Metal Research, Chinese Academy of Sciences, 72 Wenhua Road, Shenyang 110016, China*

[4]*Condensed Matter Theory Group, Physics Department, Uppsala University, Uppsala SE-75121, Sweden*

[5]*School of Physics and Optoelectronic Technology & College of Advanced Science and Technology, Dalian University of Technology, Dalian 116024, China*

[6]*Research Institute for Solid State Physics and Optics, Budapest H-1525, P.O. Box 49, Hungary*

(Received 11 December 2006; revised manuscript received 2 October 2007; published 4 December 2007)

The effect of Zr on the martensitic transformation (MT) behavior and mechanical properties of $(Ti_{0.5-x}Zr_x)Ni_{0.5}$ alloys is investigated by calculating the elastic constants and elastic moduli in the $B2$ phase as a function of x for $0 \leqslant x \leqslant 0.2$. The calculations are performed using the coherent potential approximation implemented within the framework of the exact muffin-tin orbitals method. We find that the theoretical elastic properties correlate well with the behavior of the MT. With increasing Zr concentration, the anisotropy of the alloy decreases, indicating that the nonbasal plane shear on which the modulus C_{44} plays an important role, dominates and, therefore, a monoclinic martensitic phase should result. The experimental Zr content dependence of the MT temperature is paralleled with the calculated C_{44} versus Zr content. The theoretical elastic moduli demonstrate that the (TiZr)Ni alloys, with Zr distributed randomly on the Ti sublattice, are intrinsically ductile, which suggests that the poor ductility of these alloys may be ascribed to some other factors, for example, impurities, precipitation, and grain boundaries.

DOI: 10.1103/PhysRevB.76.224201 PACS number(s): 71.20.Be, 62.20.Dc, 61.66.Dk

I. INTRODUCTION

Titanium-nickel alloys show excellent shape memory effects (SME), resulting from the reversible martensitic transformation between high-temperature $B2$ and low-temperature $B19'$, $B19$, or R phases. These materials have been widely used in robotic, automotive, aerospace, etc., industries.[1] However, due to the fact that the SME of unalloyed TiNi occurs in the temperature range from 40 to 60 °C, some applications (e.g., fire alarm) of these alloys have been greatly limited. However, materials scientists have managed to develop TiNi-based alloys[2] with higher martensitic transformation temperature.[3] Among diverse potential high temperature shape memory alloys (HTSMA), the TiNi-Zr system has drawn much attention due to the relative low cost of the raw materials. Experiments have shown that, with a small addition of Zr, the martensitic transformation temperature decreases.[4] When the concentration of the alloying element Zr exceeds 10 at. %, the martensitic transformation temperature increases to as high as 170 °C for 20.2 at. % Zr.[5,6] Substitution of Ti with Zr up to 20 at. % keeps the intial $B2$ structure, an uninterrupted range of solid solution; the martensite remains monoclinic, identical to that for unalloyed TiNi.[6] However, similar to all other HTSMAs, the TiNi-Zr alloys suffer from poor mechanical properties (e.g., low ductility), which makes the practical application of these alloys difficult.[7] Further efforts are needed to improve the mechanical properties of these alloys. The purpose of this work is to exploit theoretically the effect of Zr on the mechanical properties of TiNi alloys.

It has been recognized that the SME is closely related to the elastic instability of the high-temperature parent $B2$ phase.[8] During the martensitic transformation, $B2$-TiNi is subjected to elastic softening, i.e., the cubic elastic constants $C' = \frac{1}{2}(C_{11} - C_{12})$ and C_{44} decrease with a lowering of the temperature. C' is the modulus of the shear along the $\{110\}\langle 1\bar{1}0\rangle$ direction (basal-plane shear), whereas C_{44} is the modulus of the $\{001\}\langle 1\bar{1}0\rangle$ or $\{001\}\langle 100\rangle$ (nonbasal-plane) shear. The lattice instability due to the softening of C' of the high temperature $B2$ phase gives a reasonable explanation to the martensite structures such as $B19$ and R phases, whereas the softening of C_{44} correlates with the onset of the $B19'$ martensite structure.[9,10] The relative elastic constants of the TiNi based alloys to those of the unalloyed TiNi may be a good indication of the influence of alloying on the martensitic transformation. For example, the addition of Fe to TiNi increases both the C' and C_{44} values of the alloy, i.e., improves the dynamic stability and, consequently, lowers the martensitic transformation temperature.[10]

Inspired by the above considerations, in the present work we study the elastic properties of the TiNi-Zr alloys as a function of Zr content. A natural question that arises is the preferential location of the Zr atoms in the $B2$ structure. Experiments indicate that Zr atoms occupy the Ti sublattice.[6] From the theoretical side, the problem of site-occupancy in the Ti-Ni-Zr ternary system requires complex investigations, which are beyond the scope of the present work. Instead, here we give an argument for restricting the present elastic constant study to the Ti-deficient (TiZr)Ni alloys. First, by computing the heat of formation versus composition for al-

TABLE I. Theoretical lattice constant (Å) and bulk modulus (GPa) of hcp-Ti, fcc-Ni, and hcp-Zr, in comparison with the experimental values taken from Ref. 38.

		a	c/a	B
Ti	EMTO-CPA	2.93	1.61	94
	Expt.	2.95	1.59	105
Ni	EMTO-CPA	3.53		191
	Expt.	3.52		186
Zr	EMTO-CPA	3.23	1.62	76
	Expt.	3.23	1.59	83

loys with Zr content below 15% on both sublattices, we show that with sufficient Ti and Ni supply, alloys with Zr occupying the Ti-sublattice are the most stable configurations. Second, tracing the heat of formation in Ti-rich and Ni-rich systems, we demonstrate that in both Ni-rich and Ti-rich alloys Zr prefers the Ti sublattice. Because of that and in order to make the composition comparable with the experimental ones in Refs. [3,4,6,5], we limit our study to (TiZr)Ni solid solutions, where the Zr atoms are located exclusively on the Ti sublattice. Using the calculated elastic constants of $(Ti_{0.5-x}Zr_x)Ni_{0.5}$ alloys $(0 \leqslant x \leqslant 0.2)$, the effect of Zr on the SME as well as the mechanical properties of TiNi alloys are discussed.

The paper is arranged as follows: In Sec. II, we briefly describe the first-principles method and the parameters adopted in our calculations. Results are presented and discussed in Sec. III. First, in Sec. III A, we compare our calculated bulk properties of the pure metals and unalloyed $B2-$TiNi with other theoretical and experimental values. The site occupation of Zr is investigated in Sec. III B. The theoretical elastic constants of (TiZr)Ni alloys, calculated as a function of composition are presented in Sec. III C. Here we also discuss the influence of Zr on the martensitic transformation. In Sec. III D, we study the composition dependence of some polycrystalline elastic moduli which are relevant for the mechanical properties. Finally, the main results are summarized in Sec. IV.

II. METHOD

Theoretical determination of the elastic constants by using first-principles methods based on density functional theory[11] is now a routine matter. For instance, reasonably accurate elastic constants of TiNi have been obtained in pseudopotential calculations.[12] On the other hand, within the framework of conventional density functional methods, a direct calculation of random alloys, especially those with complex multiple concentrations, is very inconvenient. As a matter of fact, to our knowledge, no first-principles calculations of the elastic constants of TiNi-based alloys have been reported. The difficulty mentioned above has recently been resolved by implementing the coherent potential approximation (CPA) in the exact muffin-tin orbitals (EMTO) density functional method.[13] The EMTO-CPA approach ensures the accuracy needed for the calculations of both uniform and anisotropic lattice distortions.

TABLE II. Structural, cohesive, and elastic properties of unalloyed $B2$-TiNi. The results listed in the parenthesis were obtained with Ti-$3p$ semicore states treated as valence states.

	EMTO-CPA	Theoretical[a]	Experimental
Lattice constants a_0 (Å)	3.017 (3.016)	2.977	3.015[b]
Heat of formation (eV)	−0.38	−0.33	−0.35[c]
C' (GPa)	35 (34)	12	17[d]
C_{44} (GPa)	53 (51)	50	35[d]
Anisotropy $A=C_{44}/C'$	1.53	4.17	2.09[d]
Anisotropy factor $A^{-1/2}$	0.81	0.49	0.69[d]
Bulk modulus B (GPa)	157 (153)	156	140[d]
Shear modulus G (GPa)	46	35	28[d]
G/B	0.29	0.23	0.20[d]
Poisson ratio ν	0.37	0.39	0.41[d]

[a]Reference 12.
[b]Reference 40.
[c]Reference 41.
[d]Reference 39.

The EMTO method is an improved screened Korringa-Kohn-Rostoker method,[14] where the one-electron potential is represented by large overlapping muffin-tin potential spheres. By using overlapping spheres, one describes more accurately the crystal potential, when compared to the conventional nonoverlapping muffin-tin approach.[15,16] Further details about this method can be found in Refs. 13–18. The EMTO-CPA approach has been applied successfully in the theoretical study of the elastic constants and phase stability of random Fe-based alloys,[19–23] simple and transition metal alloys,[24–26] and Hume-Rothery systems,[13,28,29] as well as the crystal structure of complex oxides.[30–33]

All the calculations from the present work were carried out using the EMTO-CPA method. The exchange-correlation term was described within the generalized-gradient approximation (GGA) by Perdew *et al.*[34] The EMTO basis set included s, p, d, and f orbitals. The one-electron equations were solved within the scalar-relativistic approximation. The Ti-$3d^24s^2$, Zr-$4d^25s^2$, and Ni-$3d^84s^2$ states were treated as valence states and the core states were recalculated after each iteration. Calculations with Ti-$3p$ and Zr-$4p$ semicore states treated as valence states were also tested, and the results show (see Table II) that putting the $3p$ states into the core has negligible effect on the elastic constants. For each composition and crystal lattice, the EMTO-CPA Green function was calculated self-consistently for 16 complex energy points distributed exponentially on a semicircular contour, which included states within 1 Ry below the Fermi level. Test calculations for the unalloyed TiNi demonstrated that increasing further the number of energy points has a negligible ($\lesssim 0.01\%$) effect on the equilibrium lattice constants and elastic constants. In the one-center expansion of the full charge density, we adopted an l-cutoff of 10 and the total energy was calculated using the full charge density technique.[16]

The theoretical equilibrium volume V and bulk modulus B were determined by fitting the total energies versus volume

according to the Murnaghan equation of state.[35] To get the cubic shear constants C' and C_{44}, we used the following volume conserving orthorhombic:

$$\begin{pmatrix} 1+\epsilon_o & 0 & 0 \\ 0 & 1-\epsilon_o & 0 \\ 0 & 0 & \frac{1}{1-\epsilon_o^2} \end{pmatrix} \quad (1)$$

and monoclinic deformations

$$\begin{pmatrix} 1 & \epsilon_m & 0 \\ \epsilon_m & 1 & 0 \\ 0 & 0 & \frac{1}{1-\epsilon_m^2} \end{pmatrix}, \quad (2)$$

respectively. Note that the resulting monoclinic structure can also be described as a base centered orthorhombic lattice. The corresponding total energies $E(\epsilon_o)$ and $E(\epsilon_m)$ were computed for six strains $\epsilon=0,0.01,0.02,\ldots,0.05$. The elastic constants C' and C_{44} were obtained by fitting the total energies with respect to ϵ_o and ϵ_m as $E(\epsilon_o)=E(0)+2VC'\epsilon_o^2$ and $E(\epsilon_m)=E(0)+2VC_{44}\epsilon_m^2$, respectively.

For the Brillouin zone sampling, we used a uniform k-mesh without any smearing technique. The coherent Green function was determined for each k-point separately and the k-integrated Green function was used to find the Green functions for alloy components via the single-site approximation.[13] In order to establish the number of k points (N_k, in the irreducible Brillouin zone) needed for well-converged elastic constants, we performed a test calculation for pure TiNi. We found that by increasing N_k from ~2000 to ~9000, the two cubic shear constants changed on the average by ~2.2%. Further increase of N_k to ~15 000 had an influence below 0.2% in the elastic constants. Since the concentration dependence of C_{44} for $(Ti_{0.5-x}Zr_x)Ni$ with $x \leqslant 0.06$ is of order of 1% (see Sec. III C), we decided to use $N_k \approx 15\,000$ in the actual calculations. We note that for alloys with $x>0.10$ a significantly smaller N_k already yields well-converged elastic constants. Based on the accuracy of our Brillouin zone sampling and on the numerical errors due to the energy integration and one-center formalism,[16] we estimate the numerical error bar for the elastic constants to be below 0.3%.

The polycrystalline elastic constants were calculated using the Hill averaging method.[36] First, the C_{11} and C_{12} elastic constant were separated from the bulk modulus $B=\frac{1}{3}(C_{11}+2C_{12})$ and the tetragonal shear constant $C'=\frac{1}{2}(C_{11}-C_{12})$. Then, the polycrystalline shear modulus was calculated as the arithmetic Hill average $G=\frac{1}{2}(G_V+G_R)$, where $G_V=\frac{C_{11}-C_{12}+3C_{44}}{5}$ and $G_R=\frac{5}{4S_{11}-4S_{12}+3S_{44}}$ are the Voigt and Reuss bounds, respectively, and S_{11}, S_{12}, and S_{44} are the elastic compliances.[37] Finally, the Poisson ratio ν and Young's modulus were obtained as $\nu=\frac{1}{2}\left(\frac{3B-2G}{3B+G}\right)$ and $E=\frac{9GB}{G+3B}$, respectively.

III. RESULTS AND DICUSSIONS

A. Pure metals and unalloyed TiNi

As a test of the EMTO-CPA method, in Table I we compare the present theoretical equilibrium lattice constants and bulk moduli of elemental hexagonal close packed (hcp) Ti and Zr and face centered cubic (fcc) Ni with the corresponding experimental data.[38] The properties of Ni were calculated taking into account the spin polarization. It is seen that our results are in reasonably good agreement with the experimental values. In fact, the obtained differences can be ascribed to the typical errors associated with the GGA for the energy functional.

The structural and elastic properties as well as the heat of formation of unalloyed $B2$-TiNi are listed in Table II. For comparison, values from other theoretical calculations[12] and experiments[39–41] are also included in the table. The heat of formation was calculated from the ground state energies as

$$\Delta E = (E_{\mathrm{TiNi}} - E_{\mathrm{Ti}} - E_{\mathrm{Ni}})/2, \quad (3)$$

where E_{TiNi} is the total energy per unit cell for $B2$-TiNi, and E_{Ti} and E_{Ni} are the total energies of hcp Ti and fcc Ni, respectively. The present lattice constant is in perfect agreement with the experimental value.[40] The EMTO-CPA heat of formation is slightly smaller than the experimental value, but the error is similar to that obtained in a pseudopotential calculation.[12] Both C' and C_{44} calculated using the EMTO-CPA method are greater than the experimental values. On the other hand, the present Zener anisotropy ratio, $A=C_{44}/C'$, agrees well with experiment. Although the pseudopotential calculations by Ye *et al.*[12] give C' in a better agreement with experiment compared to our approach, the former method strongly overestimates A.

The Zener anisotropy was believed to be crucial for the martensitic transformation of TiNi.[3,8,9] In general, the Zener anisotropy of alloys undergoing martensitic transformation is quite large (>10). During the martensitic transformation, C' softens whereas C_{44} almost remains unchanged, which leads to an increasing A with decreasing temperature toward the martensitic transformation temperature, and there is little correlation between the basal-plane and nonbasal-plane shear. In this type of alloy, a conventional basal-plane shear picture is valid for the martensitic transformation. However, in the case of TiNi, the Zener anisotropy is quite small and both C' and C_{44} soften during the transformation, such that both basal-plane and nonbasal-plane shear affect the transformation and the consequent martensitic structure. That is why the martensitic phase of TiNi is monoclinic. This idea has been demonstrated by Otsuka and Ren,[9] who have shown that Cu addition increases C_{44} but decreases C', and consequently these alloys go through an orthorhombic $B19$ intermediate structure and then achieve its ultimate $B19'$ martensitic phase.

In Table II we also list some of the quantities that are closely related to the mechanical properties of solids. Both theoretical and experimental data give a relatively small shear modulus to bulk modulus ratio (G/B) for TiNi. In 1954, Pugh[42] showed that pure metals with small G/B generally have more extended deformation range and therefore

are more plastic than those with large G/B. This empirical rule is also true for intermetallic compounds as demonstrated by Fu.[43] G/B is now widely adopted as a predictor in first-principles materials design. Consistent with the experimental findings, the small G/B value of TiNi implies that the material may deform plastically. Another index for the mechanical properties of materials is the anisotropy factor $A^{-1/2}$ versus the Poisson ratio ν.[46] Materials such as the $B2$ ionic crystal (brittle) have large $A^{-1/2}$ (>1.2) and small ν (<0.3), whereas brittle $B2$ intermetallic compounds have small $A^{-1/2}$ (<0.8) and large ν (>0.35). The bcc metals have $A^{-1/2}$ and ν lying in between the two brittle systems, and therefore are more isotropic in nature (see Fig. 4 in Ref. 46). The isotropic nature of the bcc metals accounts for the ductility of these materials. From Fig. 4 in Ref. 46, it is notable that TiNi with calculated $A^{-1/2}$ of 0.81 and ν of 0.37 is located close to the bcc metals, indicating that pure TiNi is intrinsically ductile.

B. Site-occupancy of Zr in TiNi

Since there are two sublattices in $B2$-TiNi, one should first determine on which of the two sublattices the alloying atoms are located. Because Zr and Ti have similar valence states and the atomic volume of Zr differs only by 24% from that of Ti (compared to 53% difference in the case of Ni), it is expected that substituting Ti by Zr is thermodynamically more favorable than substituting Ni by Zr. Indeed, according to experiments,[6] in Zr-doped TiNi the Zr atoms occupy the Ti sublattice.

Theoretically, the question of site-occupancy can be addressed by comparing the heats of formation calculated for configurations with different site occupations. Here our purpose is to identify theoretically those systems for which the results from Secs. III C and III D are valid. Therefore instead of performing a full site-occupancy investigation for the complete Ti-Ni-Zr ternary system, we address the site occupancy for a TiNi-Zr alloy with Zr content below 30% (maximum 15% on each sublattice). First, we consider systems without Ti and Ni antisite defects. The heat of formation for $(Ti_{0.5-x}Zr_x)(Ni_{0.5-y}Zr_y)$ was calculated as

$$\Delta E(x,y) = E_{Ti_{0.5-x}Ni_{0.5-y}Zr_{x+y}} - (0.5-x)E_{Ti} - (0.5-y)E_{Ni} - (x+y)E_{Zr}, \quad (4)$$

with $E_{Ti_{0.5-x}Ni_{0.5-y}Zr_{x+y}}$ being the total energy per atom of the TiNi-Zr alloy, and E_{Ti}, E_{Ni}, and E_{Zr} being the total energies of hcp Ti, fcc Ni, and hcp Zr in their elemental state, respectively. x and y denote the atomic fractions of Zr on Ti and Ni sublattices, respectively. Obviously, more negative heat of formation indicates more favorable configuration.

Figure 1 shows the map for $\Delta E(x,y)$ calculated for $0 \leqslant x \leqslant 0.15$ and $0 \leqslant y \leqslant 0.15$. It can be seen that the heat of formation increases (decreases in absolute value) with increasing Zr concentration, following the regular solid solution model. For instance, for a homogeneous distribution of Zr ($x=y$), the heat of formation increases from −0.38 eV obtained for pure TiNi to −0.10 eV corresponding to 15% Zr doping on both sublattices. According to the figure, at normal working temperature the configurational entropy alone would be insufficient to stabilize (relative to the pure components) a solid solution where the Zr atoms are more or less uniformly distributed on both sublattices.

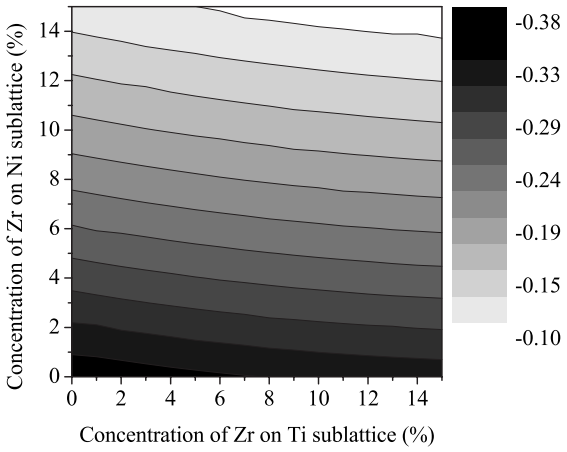

FIG. 1. Map of the heat of formation (in eV) of the (TiZr)(NiZr) system with respect to the concentrations of Zr on Ti (abscissa) and Ni (ordinate) sublattices.

For a fixed Zr content ($x+y=$const), the Ni-rich alloys (corresponding to $y \approx 0$) have lower heat of formation than the Ti-rich alloys ($x \approx 0$). Therefore with sufficient Ti and Ni supply, alloys with Zr occupying the Ti sublattice are the most stable configurations. This result is in line with experimental[6] and former theoretical[44,45] findings. What is more important, the present results from Fig. 1 demonstrate that the site-occupancy is rather independent on Zr content: $(Ti_{0.5-x}Zr_x)Ni$ is found to be the most stable alloy for any antisite-free configuration.

It is interesting to note that the trend of the heat of formation from Fig. 1 correlates well with the equilibrium volume of the alloy. The present theoretical lattice constant of $(Ti_{0.5-x}Zr_x)(Ni_{0.5-y}Zr_y)$ follows Vegard's law and can be parametrized as $a(x,y) \approx a_0 + 0.46x + 0.73y$, where a_0 is the lattice constant of pure TiNi. Accordingly, with increasing Zr content ($x+y$), the lattice constant always increases. Furthermore, for a fixed Zr content, the lattice constants of Ti-rich alloys are larger than those of Ni-rich alloys. Taking into account that, in general, with volume expansion the alloy components become less bonded and the heat of formation increases, we may draw the conclusion that the lattice expansion with Zr addition and partition partly explains the observed trend in the heat of formation.

Next, we consider the possibility of Ti and Ni antisite defects. It has recently been shown that in pure TiNi the formation of antisite defects are energetically unfavorable.[47] However, we cannot rule out the possibility that Zr addition enhances the formation of antisites. Here we investigate this question in the case of two Zr-containing systems: a Ni-rich $(Ti_{0.35}Ni_zZr_{0.15-z})(Ni_{0.50-z}Zr_z)$ and a Ti-rich $(Ti_{0.50-z}Zr_z) \times (Ni_{0.35}Ti_zZr_{0.15-z})$ solid solution. In Fig. 2, the heat of formation for both alloys are shown as a function of z. In Ni-rich alloys (squares), putting Zr atoms on the Ni sublattice leads to Ni antisites on the Ti sublattice. In this process the energy of the system raises as a result of (i) antisite defects

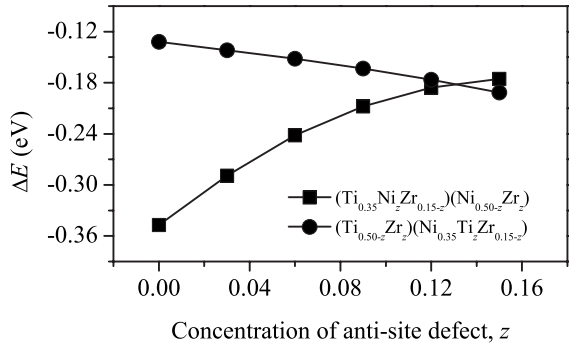

FIG. 2. Heats of formation of Ni-rich and Ti-rich TiNi-Zr alloys calculated as a function of the concentration of antisite defect: Ni on Ti sublattice (squares) and Ti on Ni sublattice (circles). $(Ti_{0.35}Ni_zZr_{0.15-z})(Ni_{0.50-z}Zr_z)$ corresponds to 35%-Ti, z-Ni, and $(15\%-z)$-Zr occupying the Ti sublattice and $(50\%-z)$-Ni and z-Zr occupying the Ni sublattice, with similar representation for $(Ti_{0.50-z}Zr_z)(Ni_{0.35}Ti_zZr_{0.15-z})$.

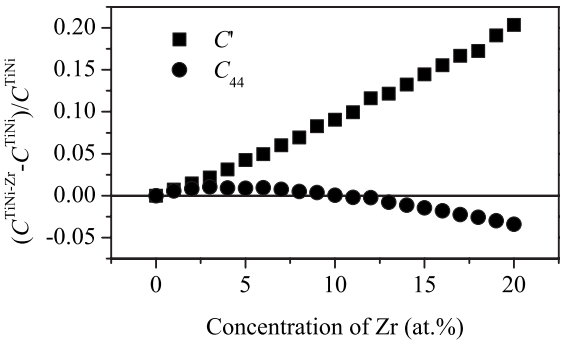

FIG. 3. Theoretical elastic constants of $(Ti_{0.5-x}Zr_x)Ni_{0.5}$ calculated as a function of Zr concentration. The two cubic elastic constant, C' and C_{44}, are plotted relative to the elastic constants of the unalloyed TiNi.

and (ii) Zr atoms occupying the energetically unfavorable Ni sites (see Fig. 1). In Ti-rich alloys (circles) the situation is completely different. The occurrence of Ti antisite raises the total energy of the system. At the same time, moving Zr from Ni sites to Ti sites lowers the total energy (see Fig. 1). If the latter effect is more pronounced than the former one, the antisite defects will occur in Ti-rich alloys. Indeed, as shown in Fig. 2 (circles), with increasing z the heat of formation slightly decreases. Therefore in Ni-rich alloys the antisites are not stable, but in Ti-rich alloys some of the Ti atoms are expelled to Ni sublattice. Namely, in both cases, Zr prefers to occupy the Ti sublattice. Since in the present work we focus only on the Ti-deficient (TiZr)Ni alloys, in the following we will consider systems without antisite defects. The effect of Zr-induced Ti antisites on the elastic properties of Ti-rich alloys remains to be investigated.

C. Effect of Zr on martensitic transformation

In this section, we study the elastic constants of $(Ti_{0.5-x}Zr_x)Ni_{0.5}$ alloys. As shown in the above section, for these systems Zr atoms occupy solely the Ti sublattice. Figure 3 shows the variations of C' and C_{44} for TiNi-Zr, relative to those of the unalloyed TiNi, as a function of Zr content. With increasing Zr concentration, $\Delta C'/C'^{\mathrm{TiNi}}$ increases monotonically, whereas $\Delta C_{44}/C_{44}^{\mathrm{TiNi}}$ slightly increases at low Zr concentration and decreases with Zr concentration for $x \gtrsim 0.06$. The corresponding Zener anisotropy is plotted in Fig. 4. We find that A decreases with Zr concentration, indicating that the coupling between C' and C_{44} becomes stronger,[9] and consequently it can be expected that the nonbasal-plane shear plays a more important role in the martensitic transformation. As we discussed in Sec. I, the nonbasal-plane shear correlates with the formation of the monoclinic martensitic phase. Therefore the martensitic phase should have monoclinic structure, in line with the experimental results.[6]

Before analyzing the effect of Zr on the properties of TiNi-Zr alloys, we first discuss the accuracy of the concentration dependence of C_{44} from Fig. 3. An obvious question that rises is whether the present theoretical approach has sufficient accuracy to resolve the small changes in C_{44} upon Zr doping. Several former applications[20,24–27] demonstrate that the EMTO-CPA method is an adequate tool in describing the nonlinear trends of the elastic properties of solid solutions, and there is no *a priori* reason why this approach should perform differently in the case of TiNi-based alloys. Regarding the present application, we paid special attention to the numerical parameters (e.g., Brillouin zone sampling, energy integration, one-center expansion) in order to keep the relative errors in the elastic constants below ~0.3%. Note that this numerical error bar is significantly smaller that the relative change calculated for C_{44} around 6% Zr. Therefore we feel confident using our theoretical elastic constants to shed light on the impact of Zr on the martensitic transformation in the TiNi-Zr system.

An impressive feature of the trend for C_{44} from Fig. 3 is that it correlates well with the martensitic transformation temperature (Ms) for these alloys. As mentioned above, with the decrease in the anisotropy, the nonbasal-plane shear may be a dominant factor for the martensitic transformation of the $(Ti_{0.5-x}Zr_x)Ni_{0.5}$ alloys. The slight increase in C_{44} with small Zr addition implies that the TiNi-Zr alloy becomes mechanically more stable compared to TiNi regarding the nonbasal-plane shear and, therefore, the martensitic transformation becomes more difficult. This should lower the martensitic transformation temperature. The above scenario is illustrated

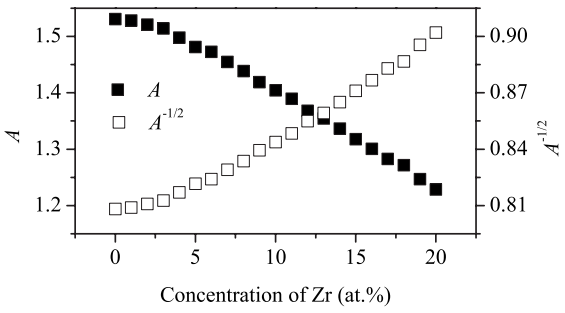

FIG. 4. Calculated Zener anisotropy of $(Ti_{0.5-x}Zr_x)Ni_{0.5}$ calculated as a function of Zr concentration.

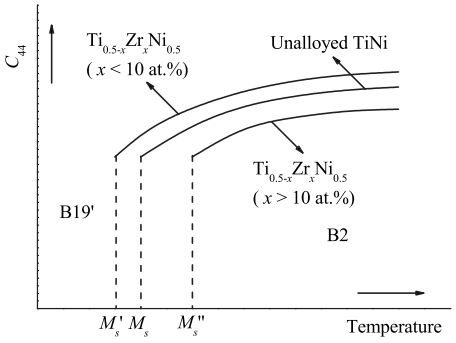

FIG. 5. Schematic representation of the alloying effect of Zr on the martensitic transformation temperature, M_s, based on the experiments from Ref. 9.

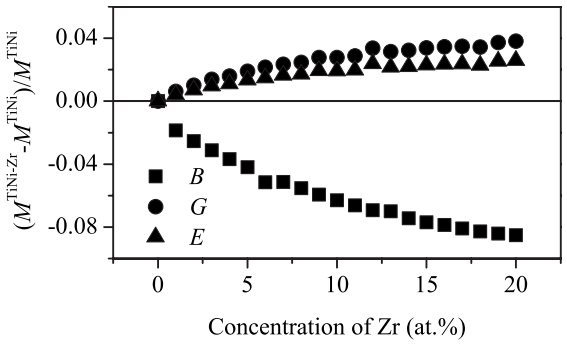

FIG. 6. Theoretical bulk modulus (squares), shear modulus (circles), and Young's modulus (triangles) of $(Ti_{0.5-x}Zr_x)Ni_{0.5}$ calculated as a function of Zr concentration. The polycrystalline elastic moduli are plotted relative to the corresponding values obtained for the unalloyed TiNi.

in Fig. 5. Our finding is in a good agreement with the recent experimental result by Feng *et al.*,[4] who have shown that with a small addition of Zr, the MT temperature is indeed lower than that of the unalloyed TiNi. However, one should also note that there are some discrepancies between different experimental measurements, which might be ascribed to the different procedures in alloy preparation. For instance, in 1976 Eckelmeyer[3] found that with 1 to 2 at. % of Zr, the MT temperature of the TiNi-Zr alloys is about 40 °C higher than that of the unalloyed TiNi.

When the concentration of Zr exceeds ~10 at. %, the calculated C_{44} becomes smaller than that of unalloyed TiNi. This means that these TiNi-Zr alloys are dynamically less stable than the host system regarding the nonbasal-plane shear. Accordingly, the MT temperature of Zr-containing TiNi alloys should be higher than that of the Zr-free system (see Fig. 5). Therefore from our calculations we predict that ~10 at. % is the critical Zr concentration for the high temperature TiNi-Zr alloys. This result is consistent with the experimental findings,[5] namely that TiNi-Zr develops high martensitic transformation temperature only when the concentration of Zr is over 10 at. %. The comparison between the calculated elastic constants of $(Ti_{0.5-x}Zr_x)Ni_{0.5}$ alloys and experimental data demonstrates that the experimental Zr-concentration dependence of the martensitic transformation temperature can be reproduced roughly by observing the variation of C_{44} with respect to the concentration of Zr. This feature has also been pointed out by Otsuka and Ren,[8] who observed that for alloys with the ultimate $B19'$ martensitic phase (although they may undergo other intermediate transformations, e.g., R and $B19$), softer C_{44} corresponds to higher transformation temperature.

D. Effect of Zr on mechanical properties

Although Zr addition above ~10 at. % increases the MT temperature of TiNi, the application of the TiNi-Zr alloys at high temperature is limited by their poor ductility. With the above calculated elastic constants, we may reexamine the relationship between Zr concentration and the mechanical properties of the TiNi-Zr alloys. The present theoretical polycrystalline elastic moduli, calculated as functions of Zr concentration, are shown in Fig. 6. Figure 7 displays the composition dependence of G/B and Poisson ratio (ν). As seen from Fig. 6, the bulk modulus decreases, while the shear and Young's moduli increase with Zr addition. This results in a slight increase in the G/B value. According to Pugh's empirical rule,[42] the increase in G/B value indicates a decrease in the ductility. However, although the G/B of the present TiNi-Zr alloys are greater than that of the unalloyed TiNi, the absolute value of G/B is still quite small. Consequently, the increase in G/B may not account for the observed poor ductility of TiNi-Zr alloys. Furthermore, although the anisotropy factor (see Fig. 4) and the Poisson ratio of the Zr-bearing alloys change with Zr concentration, they are still within the range of the pure bcc metals.[46] These results suggested that the TiNi-Zr alloys should be intrinsically ductile. The experimentally observed poor ductility of these alloys may be ascribed to some other factors, for example, impurities, precipitations, or grain boundaries.

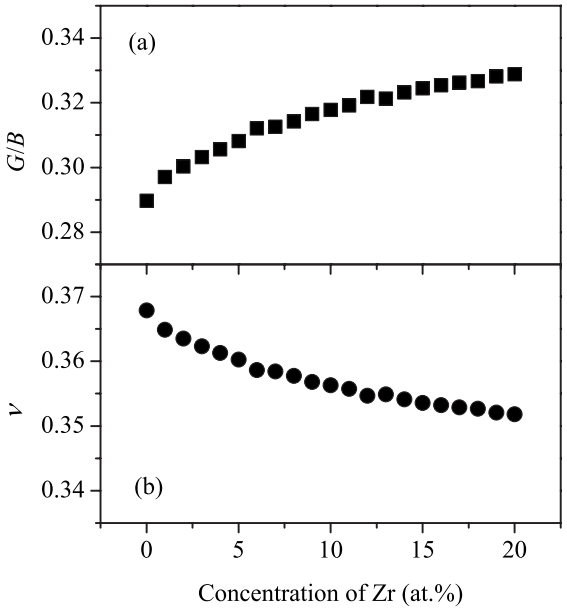

FIG. 7. Theoretical G/B (a) and Poisson ratio ν (b) of $(Ti_{0.5-x}Zr_x)Ni_{0.5}$ calculated as a function of Zr concentration.

IV. CONCLUSION

Using the first-principles EMTO method combined with the CPA, we have investigated the alloying effect of Zr on the elastic properties of Ni-rich (TiZr)Ni shaped memory alloys. The main results can be summarized in four points. (A) The Zr atoms prefer to occupy the Ti sublattice in TiNi alloys, regardless of the composition of the alloys. (B) With increasing Zr concentration, the anisotropy of $(Ti_{50-x}Zr_x)Ni_{50}$ decreases, indicating that the nonbasal-plane shear (C_{44}) dominates in the MT transformation and, therefore, a monoclinic martensitic phase should appear. (C) With increasing Zr concentration, the C_{44} elastic constant first slightly increases and then decreases, corresponding to a first decrease and then increase in the MT temperature of Zr-containing alloys. The critical Zr-concentration at which the experimental MT temperature starts to be higher than that of the unalloyed TiNi agrees very well with the Zr concentration ($\sim 10\%$) at which the calculated C_{44} drops below that of the unalloyed TiNi. (D) The calculated polycrystalline elastic moduli demonstrate that the (TiZr)Ni alloys, with Zr distributed randomly on the Ti sublattice, are intrinsically ductile. This finding suggests that the poor ductility of these alloys should be ascribed to some other factors, for example, impurities, precipitations, and grain boundaries.

ACKNOWLEDGMENTS

This work was supported by the Ministry of Science and Technology of China (Grants No. TG2000067105 and No. 2006CB605104) and Chinese Academy of Science (Grant No. INF105-SCE-02-04). Q.M.H., L.V., and B.J. acknowledge the financial support from the Swedish Research Council and the Swedish Foundation for Strategic Research. L.V. also acknowledges the financial support from the Hungarian Scientific Research Fund: research projects OTKA T046773 and T048827.

*Corresponding author. qmhu@imr.ac.cn

[1] J. Yang and Y. H. Wu, *Shape Memory Alloys and Their Applications* (Press of University of Sciences and Technology of China, Hefei, 1993) (in Chinese).

[2] In this paper, "TiNi," if not specified as "unalloyed, stoichiometric, or pure TiNi," does not necessarily refer to "equal-atomic ratio TiNi."

[3] K. H. Eckelmeyer, Scr. Metall. **10**, 667 (1976).

[4] Z. W. Feng, B. D. Gao, J. B. Wang, D. F. Qian, and Y. X. Liu, Mater. Sci. Forum **394-3**, 365 (2001).

[5] L. L. Meisner, V. P. Sivocha, and O. B. Perevalova, Physica B **262**, 49 (1999).

[6] L. Meisner and V. Sivocha, J. Phys. IV **C8**, 765 (1995).

[7] G. S. Firstov, J. van Humbeeck, and Y. N. Koval, Mater. Sci. Eng., A **378**, 2 (2004).

[8] K. Otsuka and X. Ren, Prog. Mater. Sci. **50**, 511 (2005).

[9] Xiaobing Ren and Kazuhiro Otsuka, Scr. Mater. **38**, 1669 (1998).

[10] X. Ren *et al.*, Mater. Sci. Eng., A **312**, 196 (2001).

[11] R. M. Dreizler and E. K. U. Gross, *Density Functional Theory* (Springer, Berlin, 1998).

[12] Y. Y. Ye, C. T. Chan, and K. M. Ho, Phys. Rev. B **56**, 3678 (1997).

[13] L. Vitos, I. A. Abrikosov, and B. Johansson, Phys. Rev. Lett. **87**, 156401 (2001).

[14] O. K. Andersen, O. Jepsen, and G. Krier, in *Lectures on Methods of Electronic Structure Calculations*, edited by V. Kumar, O. K. Andersen, and A. Mookerjee (World Scientific, Singapore, 1994), p. 63.

[15] O. K. Andersen, C. Arcangeli, R. W. Tank, T. Saha-Dasgupta, G. Krier, O. Jepsen, and I. Dasgupta, Mater. Res. Soc. Symp. Proc. **491**, 3 (1998).

[16] L. Vitos, Phys. Rev. B **64**, 014107 (2001).

[17] L. Vitos, H. L. Skriver, B. Johansson, and J. Kollár, Comput. Mater. Sci. **18**, 24 (2000).

[18] L. Vitos, in *Computational Quantum Mechanics for Materials Engineers* (Springer-Verlag, London, 2007).

[19] L. Vitos, P. A. Korzhavyi, and B. Johansson, Phys. Rev. Lett. **88**, 155501 (2002); Nat. Mater. **2**, 25 (2003).

[20] P. Olsson, I. A. Abrikosov, L. Vitos, and J. Wallenius, J. Nucl. Mater. **321**, 84 (2003).

[21] L. Dubrovinsky *et al.*, Nature (London) **422**, 58 (2003).

[22] L. Vitos, P. A. Korzhavyi, and B. Johansson, Phys. Rev. Lett. **96**, 117210 (2006).

[23] N. Dubrovinskaia *et al.*, Phys. Rev. Lett. **95**, 245502 (2005).

[24] A. Taga, L. Vitos, B. Johansson, and G. Grimvall, Phys. Rev. B **71**, 014201 (2005).

[25] L. Huang, L. Vitos, S. K. Kwon, B. Johansson, and R. Ahuja, Phys. Rev. B **73**, 104203 (2006).

[26] J. Zander, R. Sandström, and L. Vitos, Comput. Mater. Sci. **41**, 86 (2007).

[27] A. E. Kissavos, S. I. Simak, P. Olsson, L. Vitos, and I. A. Abrikosov, Comput. Mater. Sci. **35**, 1 (2006).

[28] B. Magyari-Köpe, G. Grimvall, and L. Vitos, Phys. Rev. B **66**, 064210 (2002).

[29] B. Magyari-Köpe, L. Vitos, and G. Grimvall, Phys. Rev. B **70**, 052102 (2004).

[30] B. Magyari-Köpe, L. Vitos, B. Johansson, and J. Kollár, Acta Crystallogr., Sect. B: Struct. Sci. **57**, 491 (2001).

[31] B. Magyari-Köpe, L. Vitos, B. Johansson, and J. Kollár, J. Geophys. Res. **107**, 1029 (2002).

[32] A. Landa, C.-C. Chang, P. N. Kumta, L. Vitos, and I. A. Abrikosov, Solid State Ionics **149**, 209 (2002).

[33] B. Magyari-Köpe, L. Vitos, G. Grimvall, B. Johansson, and J. Kollár, Phys. Rev. B **65**, 193107 (2002).

[34] J. P. Perdew, K. Burke, and M. Ernzerhof, Phys. Rev. Lett. **77**, 3865 (1996).

[35] F. D. Murnaghan, Proc. Natl. Acad. Sci. U.S.A. **30**, 244 (1944).

[36] R. Hill, Proc. Phys. Soc. London **65**, 349 (1952).

[37] G. Grimvall, *Thermophysical properties of materials* (North-Holland, Amsterdam, 1999).

[38] C. Kittel, *Introduction to Solid State Physics* (Wiley, New York, 1971).

[39] O. Mercier, K. N. Melton, G. Gremaud, and J. Hägi, J. Appl. Phys. **51**, 1833 (1980).
[40] E. Goo and R. Sinclar, Acta Metall. **33**, 1717 (1985).
[41] R. Hultgren, *Selected Values of the Thermodynamic Properties of Binary Alloys* (American Society for Metals, Metals Park, OH, 1973).
[42] S. F. Pugh, Philos. Mag. **45**, 823 (1954).
[43] C. L. Fu, J. Mater. Res. **5**, 971 (1990).
[44] D. S. Xu, Y. Song, D. Li, and Z. Q. Hu, Philos. Mag. A **75**, 1185 (1997).
[45] G. Bozzolo, R. D. Noebe, and H. O. Mosca, J. Alloys Compd. **389**, 80 (2005).
[46] K. Gschneidner *et al.*, Nat. Mater. **2**, 587 (2003).
[47] J. M. Lu, Q. M. Hu, L. Wang, Y. J. Li, D. S. Xu, and R. Yang, Phys. Rev. B **75**, 094108 (2007).